miRNA-mRNA regulatory network analysis of mesenchymal stem cell treatment in cisplatin-induced acute kidney injury identifies roles for miR-210/Serpine1 and miR-378/Fos in regulating inflammation

CHUNMEI ZHANG[1], PIYONG MA[1], ZHONGYAN ZHAO[1], NAN JIANG[1], DEDE LIAN[1], PENGFEI HUO[1] and HAILING YANG[2]

[1]Intensive Care Unit of The Emergency Department and [2]Emergency Department, China-Japan Union Hospital, Jilin University, Changchun, Jilin 130031, P.R. China

Received August 23, 2018; Accepted March 11, 2019

DOI: 10.3892/mmr.2019.10383

Abstract. The present study aimed to identify microRNAs (miRNAs) that may be crucial for the mechanism of mesenchymal stem cell (MSC) treatment in cisplatin-induced acute kidney injury (AKI) and to investigate other potential drugs that may have a similar function. Transcriptomics (GSE85957) and miRNA expression (GSE66761) datasets were downloaded from the Gene Expression Omnibus database. Differentially expressed genes (DEGs) and differentially expressed miRNAs (DEMs) were identified using the linear models for microarray data method and mRNA targets of DEMs were predicted using the miRWalk2.0 database. The crucial DEGs were screened by constructing a protein-protein interaction (PPI) network and module analysis. Functions of target genes were analyzed using the database for annotation, visualization and integrated discovery. Small molecule drugs were predicted using the connectivity map database. As a result, 5 DEMs were identified to be shared and oppositely expressed in comparisons between AKI model and control groups, and between MSC treatment and AKI model groups. The 103 DEGs were overlapped with the target genes of 5 common DEMs, and the resulting list was used for constructing the miRNA-mRNA regulatory network, including rno-miR-210/Serpine1 and rno-miR-378/Fos. Serpine1 (degree=17) and Fos (degree=42) were predicted to be hub genes according to the topological characteristic of degree in the PPI network. Function analysis indicated Serpine1 and Fos may be inflammation-related. Furthermore, gliclazide was suggested to be a potential drug for the treatment of AKI because the enrichment score was the closest to -1 (-0.9). In conclusion, it can be speculated that gliclazide may have a similar mechanism to MSC as a potential therapeutic agent for cisplatin-induced AKI, by regulating miR-210/Serpine1 and miR-378-/Fos-mediated inflammation and cell apoptosis.

Correspondence to: Dr Pengfei Huo, Intensive Care Unit of The Emergency Department, China-Japan Union Hospital, Jilin University, 126 Xiantai Street, Changchun, Jilin 130031, P.R. China
E-mail: suiyan1023@sina.com

Dr Hailing Yang, Emergency Department, China-Japan Union Hospital, Jilin University, 126 Xiantai Street, Changchun, Jilin 130031, P.R. China
E-mail: cczryhl@163.com

Key words: cisplatin, acute kidney injury, mesenchymal stem cells, microRNAs, connectivity map, small molecule drugs

Introduction

Cisplatin is one of the frequently used chemotherapeutic drugs for efficient treatment of various malignant tumors in the clinic (1). Unfortunately, patients often experience multiple serious side effects, including nephrotoxicity, neurotoxicity, cardiotoxicity, hepatotoxicity, ototoxicity, vomiting and nausea (2). Among them, acute kidney injury (AKI) represents a common adverse effect, which is estimated to occur in ~20-78% of patients undergoing cisplatin-based chemotherapy (3-6). Cisplatin can be preferentially accumulated in renal proximal tubule epithelial cells to trigger an excessive inflammatory response, oxidative stress, and then cell apoptosis and necrosis (7), all of which promote the development of acute renal failure and lead to the subsequent high mortality rates in patients. Therefore, there is an urgent demand for the discovery of effective strategies to ameliorate cisplatin-induced AKI and improve patient survival, in order to broaden the clinical application of cisplatin.

Recently, accumulating evidence has suggested that transplantation of mesenchymal stem cells (MSCs) may be a potentially effective therapy for cisplatin-induced AKI (8-10). MSCs are self-renewable multipotent progenitor cells with the potential to transdifferentiate into a variety of cell types under certain conditions, including renal proximal tubule epithelial cells (11). Thereby, MSC-based therapy, on one hand, may repair the injured renal tissues by induction of cell regeneration to replace the damage cells. On the other hand, MSCs

have immunomodulatory characteristics that promote the induction of anti-inflammatory regulatory T (Treg) cells (12), but inhibit the influx of pro-inflammatory leukocytes, macrophages, dendritic cells (DCs), neutrophils, $CD4^+$ T helper (Th), and $CD8^+$ cytotoxic T lymphocytes (CTLs) (8), leading to production of less inflammatory cytokines that cause renal cell apoptosis (12,13). Despite evidence for the therapeutic potential of MSCs (10), the clinical use of MSCs remains limited because the molecular mechanisms remain not well understood and the cost is high. Therefore, further investigation of the mechanisms of MSC therapy for AKI and exploration of drugs with similar function to MSCs are of the essence.

MicroRNAs (miRNAs) are a class of small RNAs (18-25 nucleotides) that function in regulation of cellular processes by downregulating target gene expression via binding to the 3'-untranslated region (UTR). There has been evidence to indicate that miRNAs participate in the pathogenesis of cisplatin-induced AKI (14,15). For example, Guo *et al* (16) reported that miR-709 was significantly upregulated in the proximal tubular cells of a cisplatin-induced AKI mouse model and biopsy samples of human AKI kidney tissue and correlated with the severity of kidney injury. *In vitro* experiments indicated that overexpression of miR-709 markedly induced mitochondrial dysfunction and cell apoptosis by downregulating mitochondrial transcriptional factor A (TFAM) (16). Qin *et al* (17) reported that cisplatin treatment in the rat renal proximal tubular cell line NRK-52E significantly upregulated the levels of miR-449. Inhibition of miR-449 by its sponge transfection in cisplatin-treated cells significantly promoted cell viability and suppressed cell apoptosis by downregulating acetylated p53 and BCL2 associated X (BAX) protein levels (17). Thus, regulation of miRNA/mRNA interactions may be an important mechanism underlying the functions of MSCs, or other drugs with similar function to MSCs, for treatment of cisplatin-induced AKI; however, these have been rarely validated (18,19).

The purpose of the present study was to integrate the transcriptomics expression data from a cisplatin-induced AKI rat model and the miRNA expression profiles from a cisplatin-induced AKI rat model undergoing MSC treatment, in order to screen for crucial miRNA/mRNA targets that may explain the mechanism of MSC function in AKI. The differentially expressed genes (DEGs) were also uploaded into the connectivity map (CMAP) database to identify potential drugs with similar functions to MSCs.

Materials and methods

Microarray data. Microarray datasets under accession numbers GSE85957 (20,21) and GSE66761 (18) were downloaded from the Gene Expression Omnibus (GEO) database of the National Center of Biotechnology Information (http://www.ncbi.nlm.nih.gov/geo/). The GSE85957 dataset (platform, GPL1355; Rat230_2; Affymetrix Rat Genome 230 2.0 Array) compared the gene expression profiles in kidney tissues isolated from male Han Wistar rats of AKI model induced by intraperitoneal administration of cisplatin (1 or 3 mg/kg, once) for 3, 5, 8 and 26 days (n=38) and controls (n=19). The GSE66761 dataset (platform, GPL14860; Agilent-031189 Unrestricted_Rat_miRNA_v16.0_Microarray) compared the miRNA expression profiles in kidney tissues isolated from male Sprague-Dawley control rats (n=2), AKI model induced by administration of 6 mg/kg cisplatin for 24 h (n=3) and treatment group with MSCs for 4 days (n=3). The successful establishment of the AKI model was confirmed by chemistry parameters (increased serum creatinine) and histopathological examination (18,20,21). MSCs were identified by the expression of typical surface markers (positive for CD29, CD44 and CD90, but negative for CD45) and their osteogenic and adipogenic differentiation abilities (18).

Data preprocessing and identification of DEGs and differentially expressed miRNAs (DEMs). The raw CEL files were preprocessed and normalized using the robust multichip average (RMA) algorithm (22) in the R Bioconductor affy package (version 3.4.1; http://www.bioconductor.org/packages/release/bioc/html/affy.html). The DEGs between AKI and control groups, and the DEMs between AKI, control, and MSC treatment groups, were identified using the linear models for microarray (LIMMA) method (23) in the Bioconductor R package (http://www.bioconductor.org/packages/release/bioc/html/limma.html). $P<0.05$ and $|\log FC \text{ (fold change)}| > 0.5$ were set as the cut-off points for screening the DEGs and DEMs. Bidirectional hierarchical clustering heatmaps of DEGs and DEMs were constructed using the R package pheatmap (version, 1.0.8; http://cran.r-project.org/web/packages/pheatmap/index.html).

Protein-protein interaction (PPI) network construction. The DEGs were mapped into the PPI data extracted from the search tool for the retrieval of interacting genes (STRING; version 10.0; http://string-db.org/) database (24) to obtain the interaction pairs of DEGs which were then used to construct the PPI network using the Cytoscape software (version 3.6.1; www.cytoscape.org/) (25). The topological characteristic of degree [the number of edges (interactions) of a node (protein)] was calculated and plotted with ggplot2 in R package to screen hub genes. To identify functionally related genes from the PPI network, module analysis was then performed by using the Molecular Complex Detection (MCODE) plugin of Cytoscape software with default parameters (ftp://ftp.mshri.on.ca/pub/BIND/Tools/MCODE) (26). Significant modules were defined as k-core ≥4 and nodes ≥6.

miRNA-target gene regulatory network. The related target genes of DEMs were predicted using the miRWalk database (version 2.0; http: //zmf.umm.uni-heidelberg.de/apps/zmf/mirwalk2) (27). Then, the target genes of DEMs were overlapped with the DEGs to obtain the negative relationships between DEMs and DEGs, which was used to construct the miRNA-target gene regulatory network using the Cytoscape software (version 3.6.1; www.cytoscape.org/) (25).

Function enrichment analysis. Kyoto encyclopedia of genes and genomes (KEGG) pathway and Gene ontology (GO) enrichment analyses were performed in order to explore the underlying functions of all DEGs, genes in PPI network and modules using The Database for Annotation, Visualization and Integrated Discovery (DAVID) (version 6.8;

Table I. Differentially expressed genes and miRNAs.

A, AKI model vs. control

Gene	logFC	P-value
Lingo4	-0.69	$6.96x10^{-10}$
Sytl3	-0.53	$3.80x10^{-7}$
Rnf125	-0.73	$7.57x10^{-7}$
Arntl	-0.63	$4.69x10^{-6}$
Epha4	-0.64	$6.25x10^{-6}$
LOC685158	-1.72	$6.33x10^{-6}$
Mlc1	-0.73	$2.07x10^{-5}$
Kl	-0.56	$2.21x10^{-35}$
Ptgs2	-0.61	$6.12x10^{-3}$
Atg	-0.71	$06.11x10^{-3}$
Nr1d1	1.44	$9.16x10^{-11}$
Egr1	1.48	$3.47x10^{-10}$
Cdkn1a	1.82	$4.84x10^{-10}$
Plk2	1.48	$1.46x10^{-9}$
Ccng1	0.99	$4.49x10^{-9}$
Fos	1.47	$8.70x10^{-9}$
Cxcl10	0.59	$1.18x10^{-5}$
Serpine1	0.97	$3.97x10^{-5}$
Timp1	0.73	$7.37x10^{-3}$
Ccl2	0.52	$9.79x10^{-4}$

B, AKI model vs. control

miRNA	logFC	P-value
rno-let-7b	-0.58	$6.22x10^{-45}$
rno-miR-3545-3p	-6.45	$3.27x10^{-7}$
rno-miR-466b-2*	-4.07	$2.29x10^{-6}$
rno-miR-598-3p	-6.05	$1.99x10^{-5}$
rno-miR-192*	-6.03	$2.77x10^{-5}$
rno-miR-192	-0.75	$1.19x10^{-4}$
rno-miR-218	-0.68	$5.85x10^{-4}$
rno-miR-210	-0.67	$3.60x10^{-2}$
rno-miR-99a*	-4.72	$4.39x10^{-2}$
rno-miR-378	-0.53	$4.91x10^{-2}$
rno-miR-21*	71.49	$4.89x10^{-6}$
rno-miR-132	47.91	$1.67x10^{-5}$
rno-miR-455	41.03	$2.68x10^{-5}$
rno-miR-222	34.50	$4.54x10^{-5}$
rno-let-7i	15.97	$4.75x10^{-4}$
rno-miR-21	15.22	$5.50x10^{-4}$
rno-miR-494	12.86	$9.15x10^{-4}$
rno-miR-34a	12.55	$9.84x10^{-4}$
rno-miR-18a	12.18	$1.08x10^{-3}$
rno-miR-146b	11.53	$1.27x10^{-3}$

C, MSC treatment vs. AKI

miRNA	logFC	P-value
rno-miR-146b	-1.06	$4.01x10^{-4}$
rno-miR-29b	-0.57	$1.13x10^{-2}$
rno-miR-182	-0.82	$1.24x10^{-2}$
rno-miR-103	-0.58	$1.46x10^{-2}$
rno-miR-107	-0.67	$1.74x10^{-2}$
rno-miR-203	-0.95	$2.27x10^{-2}$
rno-miR-183	-1.04	$2.74x10^{-2}$
rno-miR-132	-0.56	$3.01x10^{-2}$
rno-miR-322	-1.13	$3.68x10^{-2}$
rno-miR-22*	-0.52	$4.37x10^{-2}$
rno-miR-125b-5p	0.53	$1.87x10^{-5}$
rno-miR-532-5p	0.91	$2.25x10^{-4}$
rno-miR-142-3p	1.12	$1.08x10^{-3}$
rno-miR-222	1.50	$1.44x10^{-3}$
rno-miR-199a-5p	0.97	$1.54x10^{-3}$
rno-miR-145	0.55	$2.14x10^{-3}$
rno-miR-221	0.77	$2.37x10^{-3}$
rno-miR-378	0.58	$1.25x10^{-2}$
rno-miR-210	1.11	$1.62x10^{-2}$
rno-miR-99a*	4.03	$4.77x10^{-2}$

miRNA, microRNA; AKI, acute kidney injury; MSC, mesenchymal stem cells; FC, fold change. Top differentially expressed or crucial genes/miRNAs are listed.

http://david.abcc.ncifcrf.gov). P<0.05 was selected as the threshold to determine the significant enrichment for GO terms and KEGG pathways.

Screening of small molecule drugs similar to MSC treatment. The DEGs were uploaded into the CMAP database (http://www.broadinstitute.org/cmap/) to identify potential drugs associated with these DEGs with the threshold values of P<0.05 and |mean|>0.4. An enrichment score close to +1 indicated that the corresponding small molecules induced a similar expression profile of DEGs, while an enrichment score close to -1 suggested that the corresponding small molecules reversed the expression of DEGs.

Results

Identification of DEGs between the AKI model and control groups. Following preprocessing, a total of 388 DEGs were identified between AKI model and control, including 153 downregulated [prostaglandin-endoperoxide synthase 2 (Ptgs2); angiotensinogen (Agt)] and 235 upregulated genes [serpin family E member 1 (Serpine1); C-C motif chemokine ligand 2 (Ccl2); Fos proto-oncogene AP-1 transcription factor subunit (Fos); FosB proto-oncogene AP-1 transcription factor subunit (FosB); C-X-C motif chemokine ligand 10 (Cxcl10); TIMP metallopeptidase inhibitor 1 (Timp1)]. The expression profiles of the most notable DEGs (as determined by subsequent PPI, function enrichment and miRNA network analyses) are presented in Table I. Heat map analysis revealed that these DEGs accurately distinguished the samples into two groups (Fig. 1).

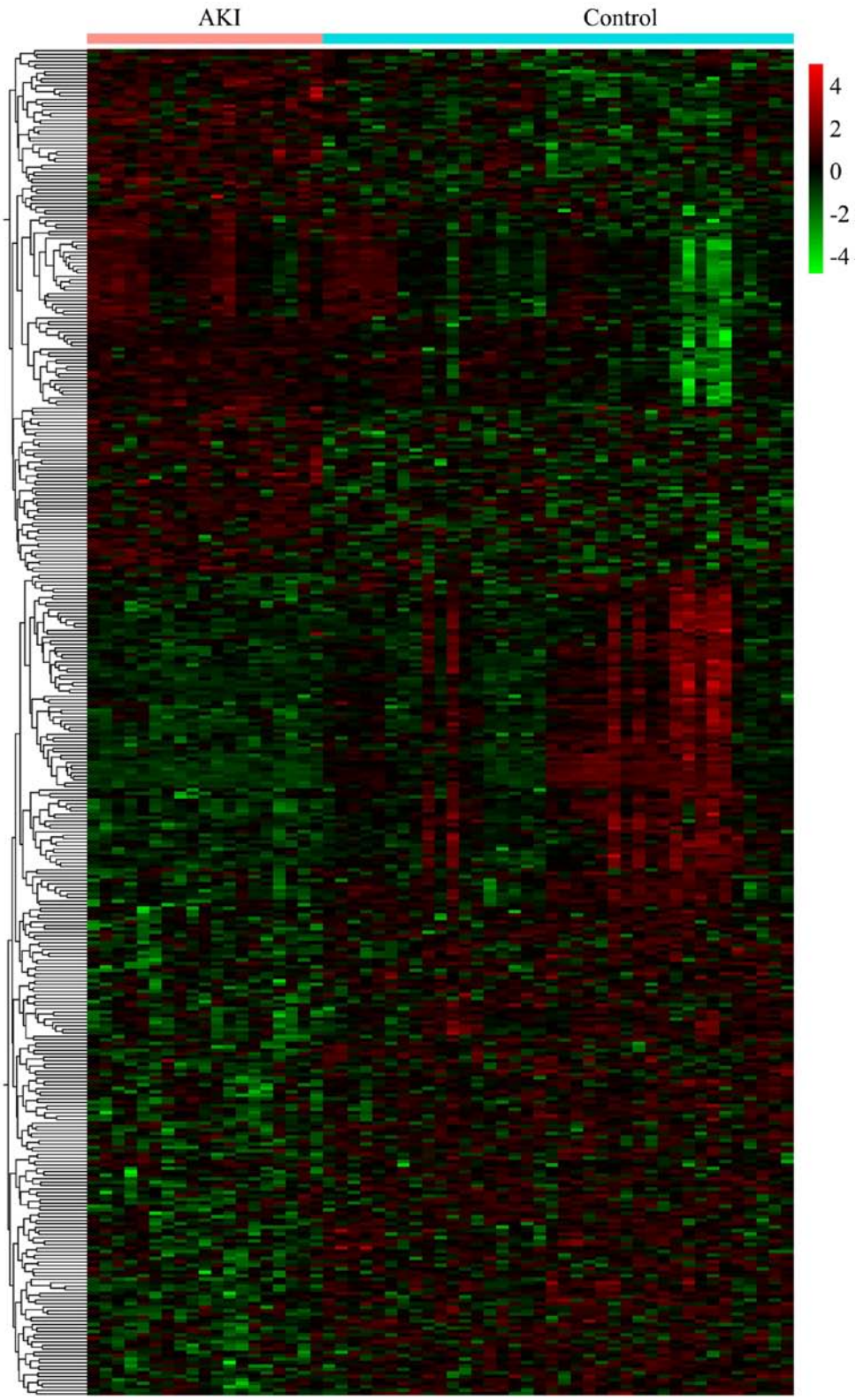

Figure 1. Hierarchical clustering heatmap analysis of differentially expressed genes between AKI model and control rats. Red, high expression; green, low expression. AKI, acute kidney injury.

Functional enrichment analysis for DEGs between the AKI model and control groups. The downregulated DEGs were significantly enriched into 7 KEGG pathways (e.g. renin-angiotensin system) and 57 GO biological process terms (e.g. response to drug; positive regulation of cell proliferation). The upregulated DEGs were significantly enriched into 12 KEGG pathways (e.g. p53 signaling pathway, amphetamine addiction, cytokine-cytokine receptor interaction) and 161 GO biological process terms (e.g. cellular response to fibroblast growth factor stimulus, negative regulation of endothelial cell apoptotic process, response to drug, positive regulation of monocyte chemotaxis, negative regulation of apoptotic

Table II. Function enrichment analysis for the upregulated and downregulated differentially expressed genes.

A, Downregulated

Category	Term	P-value	Genes involved
KEGG	rno04614:Renin-angiotensin system	$1.94x10^{-3}$	PREP, KLK1C8, AGT, MAS1
KEGG	rno04726:Serotonergic synapse	$2.77x10^{-3}$	ALOX15, CYP2D5, PTGS2, ALOX12E, GNG13, CYP2C11
KEGG	rno00590:Arachidonic acid metabolism	$2.54x10^{-2}$	ALOX15, PTGS2, ALOX12E, CYP2C11
KEGG	rno01230:Biosynthesis of amino acids	$2.70x10^{-2}$	SDS, OTC, SDSL, PGAM2
KEGG	rno00290:Valine, leucine and isoleucine biosynthesis	$3.10x10^{-2}$	SDS, SDSL
KEGG	rno00260:Glycine, serine and threonine metabolism	$3.72x10^{-2}$	SDS, SDSL, PGAM2
KEGG	rno00270:Cysteine and methionine metabolism	$3.90x10^{-2}$	SDS, SDSL, CDO1
GO BP	GO:0040018~positive regulation of multicellular organism growth	$1.96x10^{-3}$	DRD2, AGT, ATP8A2, HMGA2
GO BP	GO:0042493~response to drug	$2.04x10^{-2}$	TNFRSF11B, DAB1, CYP1A1, CRYAA, PTGS2, SFRP2, DRD2, OTC, SNCA, MAS1, SLCO1A6
GO BP	GO:0008284~positive regulation of cell proliferation	$4.94x10^{-3}$	ALOX15, KLK1C9, IL5, PTGS2, SFRP2, AGT, HLX, MAS1, TFF2, HMGA2
GO BP	GO:0030308~negative regulation of cell growth	$7.78x10^{-3}$	SFRP2, AGT, TRO, EAF2, SLIT3
GO BP	GO:0008285~negative regulation of cell proliferation	$1.02x10^{-2}$	FEZF2, PLK5, GTPBP4, PTGS2, SFRP2, DRD2, AGT, SLIT3

B, Upregulated

Category	Term	P-value	Genes involved
KEGG	rno04115:p53 signaling pathway	$2.22x10^{-4}$	CDKN1A, BBC3, SERPINE1, MDM2, SFN, CCNG1, GTSE1
KEGG	rno05166:HTLV-I infection	$9.41x10^{-4}$	ZFP36, EGR1, WNT10A, FOS, CDKN1A, ATF3, EGR2, RT1-M6-1, MYC, FOSL1, RT1-T24-4, RT1-N2
KEGG	rno00140:Steroid hormone biosynthesis	$3.30x10^{-3}$	CYP2B3, AKR1C3, UGT2B17, HSD3B1, CYP1B1, CYP3A9
KEGG	rno04512:ECM-receptor interaction	$4.94x10^{-3}$	LAMB3, COL6A5, LAMC2, SV2B, THBS3, SPP1
KEGG	rno05031:Amphetamine addiction	$8.15x10^{-3}$	FOS, STX1A, TH, FOSB, GRIN3A
KEGG	rno04610:Complement and coagulation cascades	$1.22x10^{-2}$	FGG, FGA, FGB, SERPINE1, LOC100911545
KEGG	rno04060:Cytokine-cytokine receptor interaction	$1.80x10^{-2}$	OSM, CCL2, CLCF1, TNFRSF12A, CCR2, TNFRSF8, TNFRSF4, CXCL10
KEGG	rno00590:Arachidonic acid metabolism	$1.82x10^{-2}$	CYP2B3, GPX2, ALOX5, PLA2G4B, PLA2G2D
KEGG	rno05169:Epstein-Barr virus infection	$2.29x10^{-2}$	CDKN1A, ENTPD8, MDM2,RT1-M6-1, HSPA1B, MYC, RT1-T24-4, RT1-N2
KEGG	rno05204:Chemical carcinogenesis	$2.66x10^{-2}$	CYP2B3, UGT2B17, CYP1B1, CYP3A9, GSTP1
KEGG	rno04913:Ovarian steroidogenesis	$3.24x10^{-2}$	HSD3B1, CYP1B1, ALOX5, PLA2G4B
KEGG	rno05206:MicroRNAs in cancer	$3.28x10^{-2}$	CDKN1A, CYP1B1, ABCB1A, MDM2, CCNG1, MYC

Table II. Continued.

B, Upregulated

Category	Term	P-value	Genes involved
GO BP	GO:0042493~response to drug	$5.75x10^{-7}$	EGR1, CYP2B3, HAVCR1, HSD3B1, CCL2, TH, FOSB, CPS1, RAD54L, JUNB, LCN2, FOS, SLC1A2, CDKN1A, HMGCS2, ABCB1A, TGIF1, MDM2, ABCC2, FOSL1, MYC
GO BP	GO:0032496~response to lipopolysaccharide	$3.53x10^{-5}$	CCL2, TH, TNFRSF8, CPS1, TNFRSF4, JUNB, CXCL10, FOS, UGT2B17, PDE5A, SERPINE1, CNR2, NKX2-1
GO BP	GO:0044344~cellular response to fibroblast growth factor stimulus	$6.92x10^{-5}$	ZFP36, CCL2, HSD3B1,SERPINE1, CPS1, MYC
GO BP	GO:2000352~negative regulation of endothelial cell apoptotic process	$2.44x10^{-4}$	FGG, FGA, FGB, SERPINE1, ANGPTL4
GO BP	GO:0090026~positive regulation of monocyte chemotaxis	$7.87x10^{-4}$	CCL2, SERPINE1, CCR2, CXCL10
GO BP	GO:0043066~negative regulation of apoptotic process	$9.74x10^{-4}$	IER3, CLU, HSPA1B, IL24, CCNG1, TIMP1, CDKN1A, PLK2, BTG2, MDM2, POU4F1, NQO1, FOXE3, ANGPTL4, CYR61
GO BP	GO:0006954~inflammatory response	$3.79x10^{-3}$	CCL2, CCR2, CNR2, TNFRSF8, IL24, ALOX5, ADAM8, TNFRSF4, SPP1, CXCL10
GO BP	GO:0034097~response to cytokine	$1.94x10^{-2}$	FOS, SERPINE1, FOSL1, JUNB, TIMP1

KEGG, kyoto encyclopedia of genes and genomes; GO, gene ontology; BP, biological process. Top enriched terms or terms enriched by crucial genes are listed.

process, response to cytokine). The results from the enrichment analysis, including the most notable KEGG pathways and GO processes as determined by their association with key genes, are presented in Table II.

PPI network and module analyses for DEGs between the AKI model and control groups. A total of 456 PPI pairs (e.g. Ccl2-Cxcl10, Cxcl10-Ptgs2, Agt-Cxcl10, Timp1-Fos, Agt-Timp1, Timp1-Ptgs2) were predicted from the STRING database after uploading the DEGs, which were used for constructing the PPI network, including 74 downregulated and 123 upregulated nodes (Fig. 2). The hub proteins in the PPI network were screened by computing the degree (Fig. 3A). The results revealed that Fos (degree=42), Ptgs2 (degree=33), Agt (degree=28), Ccl2 (degree=20), Serpine1 (degree=17), Timp1 (degree=15), FosB (degree=12) and Cxcl10 (degree=10) may be hub genes for AKI.

From the PPI network, only one significant module was screened (Fig. 3B). The hub genes of this module included Ptgs2, Agt, Serpine1, Ccl2 and Timp1. Functional enrichment analyses revealed that the genes in this module were involved multiple processes, including cellular response to fibroblast growth factor stimulus (Serpine1, Ccl2), inflammatory response (Ccl2, Ptgs2), response to cytokine (Serpine1, Ptgs2, Timp1), positive regulation of cell proliferation (Ptgs2, Agt, Timp1), and negative regulation of neuron apoptotic process (Ccl2, Agt; Table III).

DEMs identification. A total of 56 DEMs (29 downregulated and 21 upregulated miRNAs) were identified between AKI model and control groups (Table I), while 40 DEMs (10 downregulated and 30 upregulated miRNAs) were identified between the MSC treatment and AKI groups. After comparing the downregulated DEMs in AKI group with the upregulated DEMs in MSC treatment group, 3 common miRNAs (rno-miR-378, rno-miR-210 and rno-miR-99a*) were obtained. Comparison of the upregulated DEMs in the AKI group with the downregulated DEMs in the MSC treatment group detected 2 common miRNAs (rno-miR-146b and rno-miR-132). These findings suggested these 5 miRNAs were crucial for the development of AKI and that they could be reversed following MSC treatment. Heat map analysis revealed that these miRNAs could obviously distinguish the AKI from the control and MSC treatment groups (Fig. 4).

miRNA-target gene regulatory network analysis. Using the miRWalk2.0 database, 5,920 target genes of 56 DEMs between AKI and control were predicted, which were then

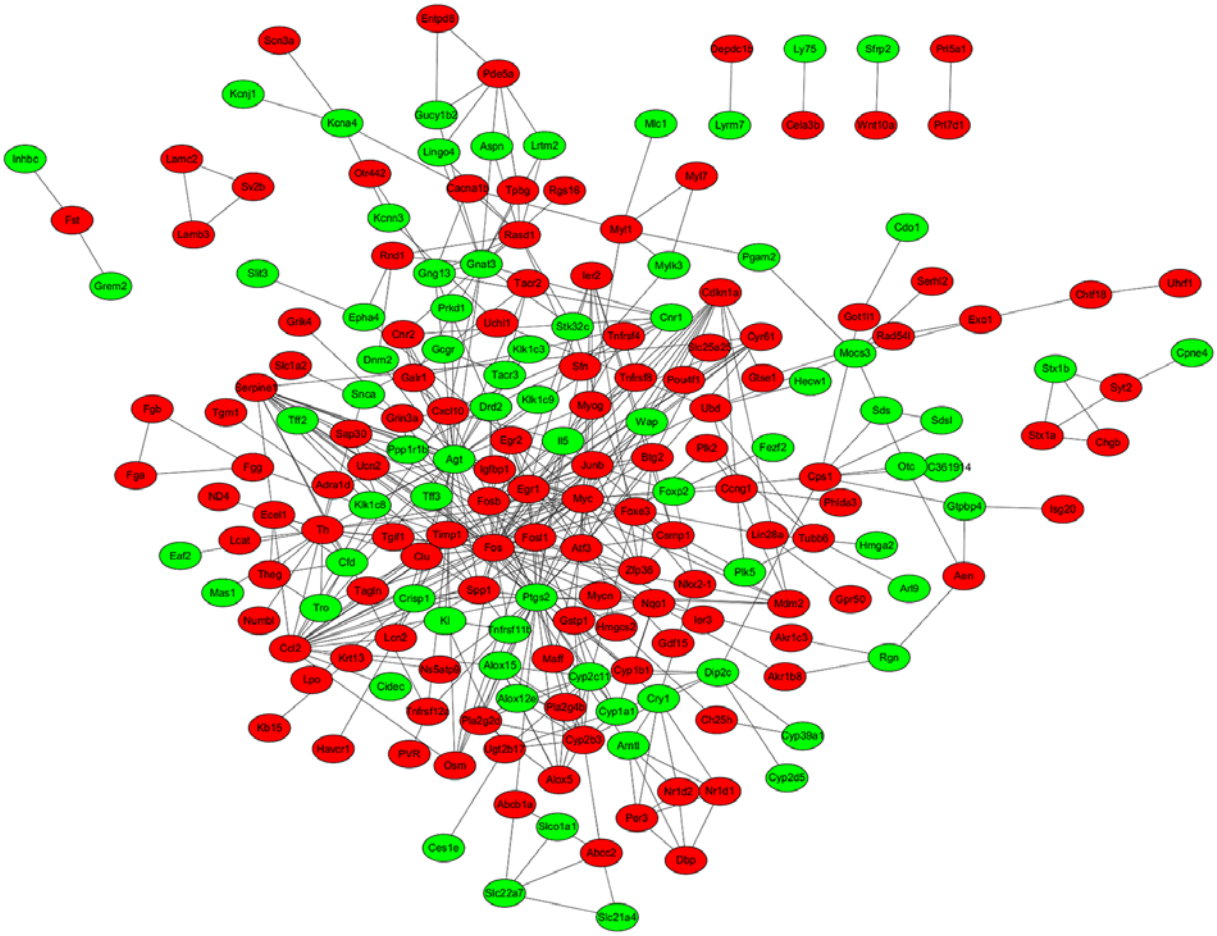

Figure 2. Protein-protein interaction network using the common differentially expressed genes. Red, upregulated; green, downregulated.

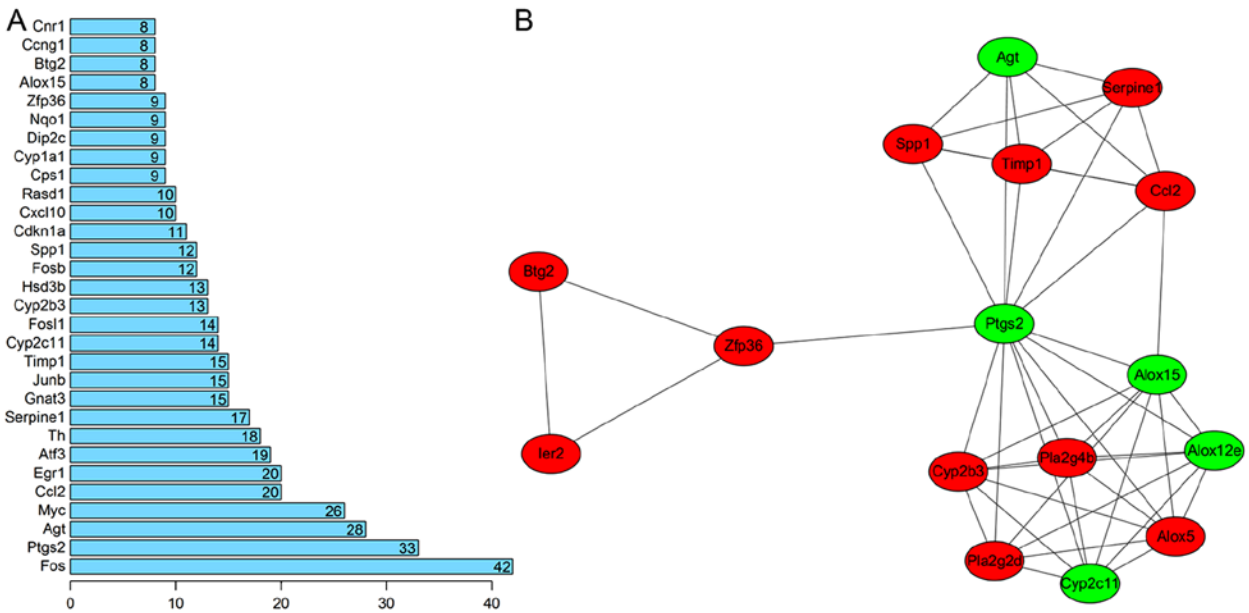

Figure 3. (A) Crucial genes extracted according to the rank of degree for each gene. (B) Functionally related module analysis. Red nodes, upregulated; green nodes, downregulated.

overlapped with the 388 DEGs, resulting in 107 common genes (46 upregulated and 61 downregulated). These 107 common genes and their related 8 miRNAs were used to construct the AKI-related DEM-target gene regulatory network (Fig. 5), including 206 interaction pairs (e.g. rno-miR-1224/Cxcl10; rno-miR-1224/Timp1; rno-miR-17-5p/FosB).

Table III. Function enrichment analysis for the genes in module.

Category	Term	P-value	Genes involved
KEGG	rno00590:Arachidonic acid metabolism	$3.30x10^{-11}$	CYP2B3, ALOX15, PTGS2, ALOX12E, ALOX5, CYP2C11, PLA2G4B, PLA2G2D
KEGG	rno04726:Serotonergic synapse	$1.69x10^{-6}$	ALOX15, PTGS2, ALOX12E, ALOX5, CYP2C11, PLA2G4B
KEGG	rno00591:Linoleic acid metabolism	$4.75x10^{-5}$	ALOX15, CYP2C11, PLA2G4B, PLA2G2D
KEGG	rno01100:Metabolic pathways	$4.01x10^{-3}$	CYP2B3, ALOX15, PTGS2, ALOX12E, ALOX5, CYP2C11, PLA2G4B, PLA2G2D
KEGG	rno04913:Ovarian steroidogenesis	$4.38x10^{-3}$	PTGS2, ALOX5, PLA2G4B
KEGG	rno05204:Chemical carcinogenesis	$1.12x10^{-2}$	CYP2B3, PTGS2, CYP2C11
KEGG	rno04750:Inflammatory mediator regulation of TRP channels	$1.76x10^{-2}$	ALOX12E, CYP2C11, PLA2G4B
KEGG	rno00592:alpha-Linolenic acid metabolism	$4.41x10^{-2}$	PLA2G4B, PLA2G2D
GO BP	GO:0044344~cellular response to fibroblast growth factor stimulus	$5.77x10^{-4}$	ZFP36, CCL2, SERPINE1
GO BP	GO:0055114~oxidation-reduction process	$1.85x10^{-3}$	CYP2B3, PTGS2, ALOX12E, ALOX5, CYP2C11
GO BP	GO:0006954~inflammatory response	$1.88x10^{-3}$	CCL2, PTGS2, ALOX5, SPP1
GO BP	GO:0034097~response to cytokine	$3.16x10^{-3}$	PTGS2, SERPINE1, TIMP1
GO BP	GO:0043524~negative regulation of neuron apoptotic process	$7.84x10^{-3}$	CCL2, BTG2, AGT
GO BP	GO:0008284~positive regulation of cell proliferation	$8.26x10^{-3}$	ALOX15, PTGS2, AGT, TIMP1
GO BP	GO:0071222~cellular response to lipopolysaccharide	$8.73x10^{-3}$	ZFP36, CCL2, SERPINE1
GO BP	GO:0090026~positive regulation of monocyte chemotaxis	$1.53x10^{-2}$	CCL2, SERPINE1
GO BP	GO:0032496~response to lipopolysaccharide	$2.33x10^{-2}$	CCL2, PTGS2, SERPINE1
GO BP	GO:0034612~response to tumor necrosis factor	$3.00x10^{-2}$	CCL2, PTGS2
GO BP	GO:0055093~response to hyperoxia	$3.62x10^{-2}$	SERPINE1, ALOX5
GO BP	GO:0045429~positive regulation of nitric oxide biosynthetic process	$3.78x10^{-2}$	PTGS2, AGT
GO BP	GO:0045907~positive regulation of vasoconstriction	$3.78x10^{-2}$	PTGS2, ALOX5
GO BP	GO:0008285~negative regulation of cell proliferation	$4.00x10^{-2}$	BTG2, PTGS2, AGT
GO BP	GO:0030593~neutrophil chemotaxis	$4.85x10^{-2}$	CCL2, SPP1

KEGG, Kyoto encyclopedia of genes and genomes; GO, Gene ontology; BP, biological process. Top enriched terms or terms enriched by crucial genes are listed.

Furthermore, 5,646 target genes were predicted for the 5 common DEMs in AKI and MSC treatment groups, which were then also overlapped with the 388 DEGs, resulting in 103 common genes (44 upregulated and 59 downregulated). These 103 common genes and their related 5 miRNAs were used to construct the MSC treatment-related DEM-target gene regulatory network (Fig. 6), consisting of 180 interaction pairs (e.g. rno-miR-210/Serpine1; rno-miR-378/Fos).

Functional enrichment analyses for genes in miRNA-target gene regulatory network. The functions of the genes in the AKI and MSC-related miRNA-target gene regulatory networks were also evaluated by GO and KEGG enrichment analyses using DAVID. As listed in Table IV, the target genes in AKI network were significantly enriched in 6 KEGG pathways (e.g. cocaine addiction and amphetamine addiction) and 53 GO BP terms (e.g. positive regulation of cell proliferation). As presented in Table V, the target genes in MSC network were significantly enriched in 3 KEGG pathways (e.g. HTLV-I infection) and 63 GO BP terms (e.g. negative regulation of cell migration, response to drug, response to lipopolysaccharide); the GO BP terms with the most

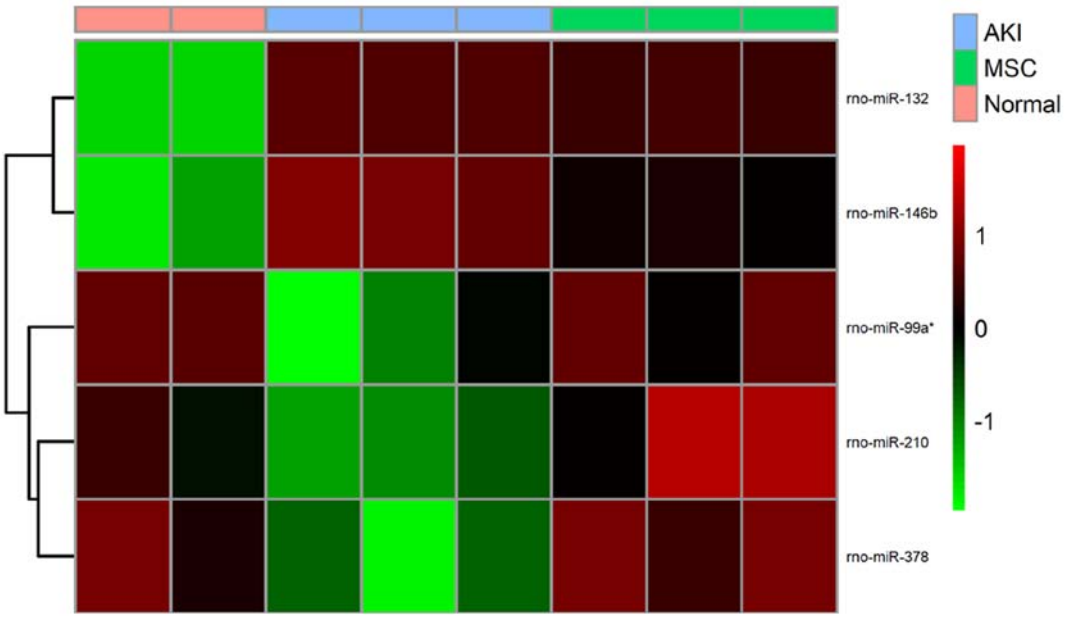

Figure 4. Hierarchical clustering heatmap analysis of common differentially expressed miRNAs. The miRNAs were inversely expressed between AKI vs. controls and MSC vs. AKI groups. Red nodes, high expression; green nodes, low expression. miRNA, microRNA; AKI, acute kidney injury; MSC, mesenchymal stem cell.

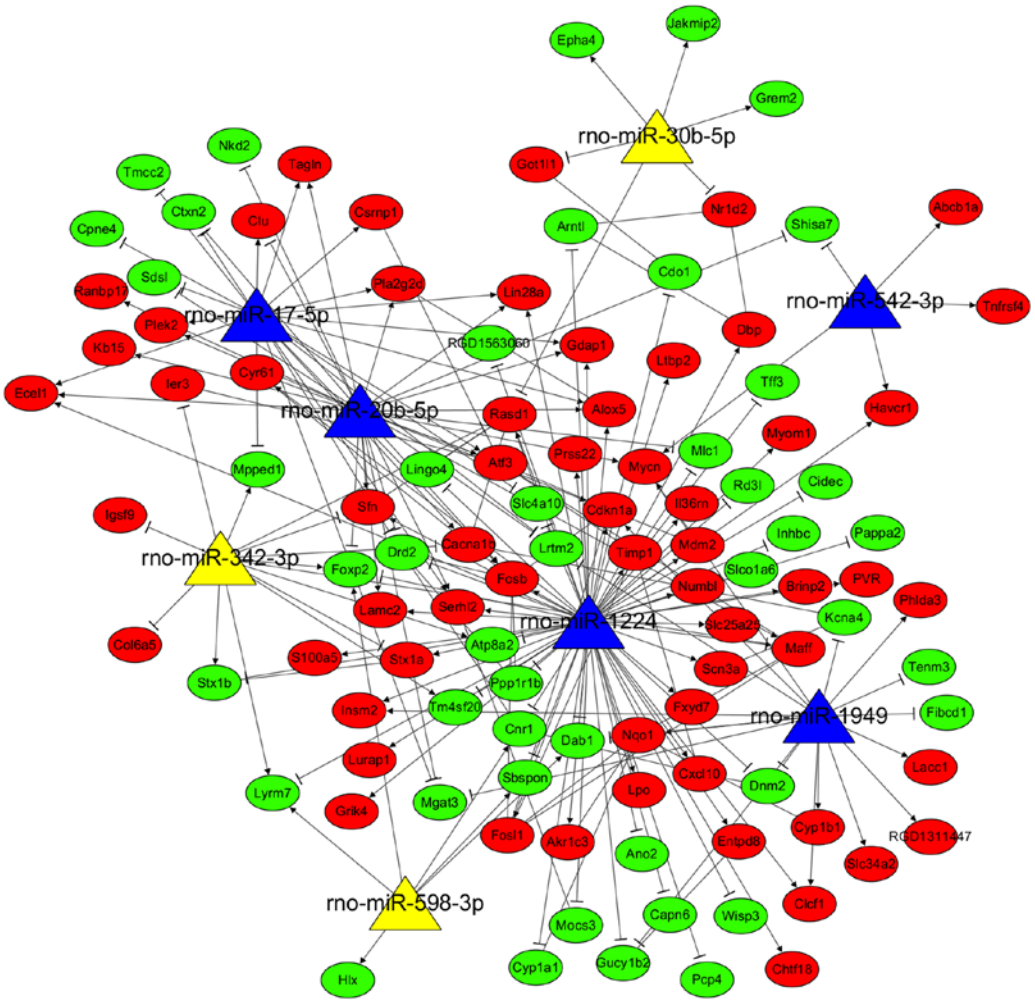

Figure 5. AKI-associated miRNA-mRNA interaction network. This network was constructed using the common genes of differentially expressed genes and the target genes of differentially expressed miRNAs. Red, upregulated genes; green, downregulated genes; yellow, upregulated miRNAs; blue, downregulated miRNAs. Arrows indicate similar expression trends between miRNAs and target genes, while lines indicate opposite expression trends between miRNAs and target genes. AKI, acute kidney injury; miRNA, microRNA.

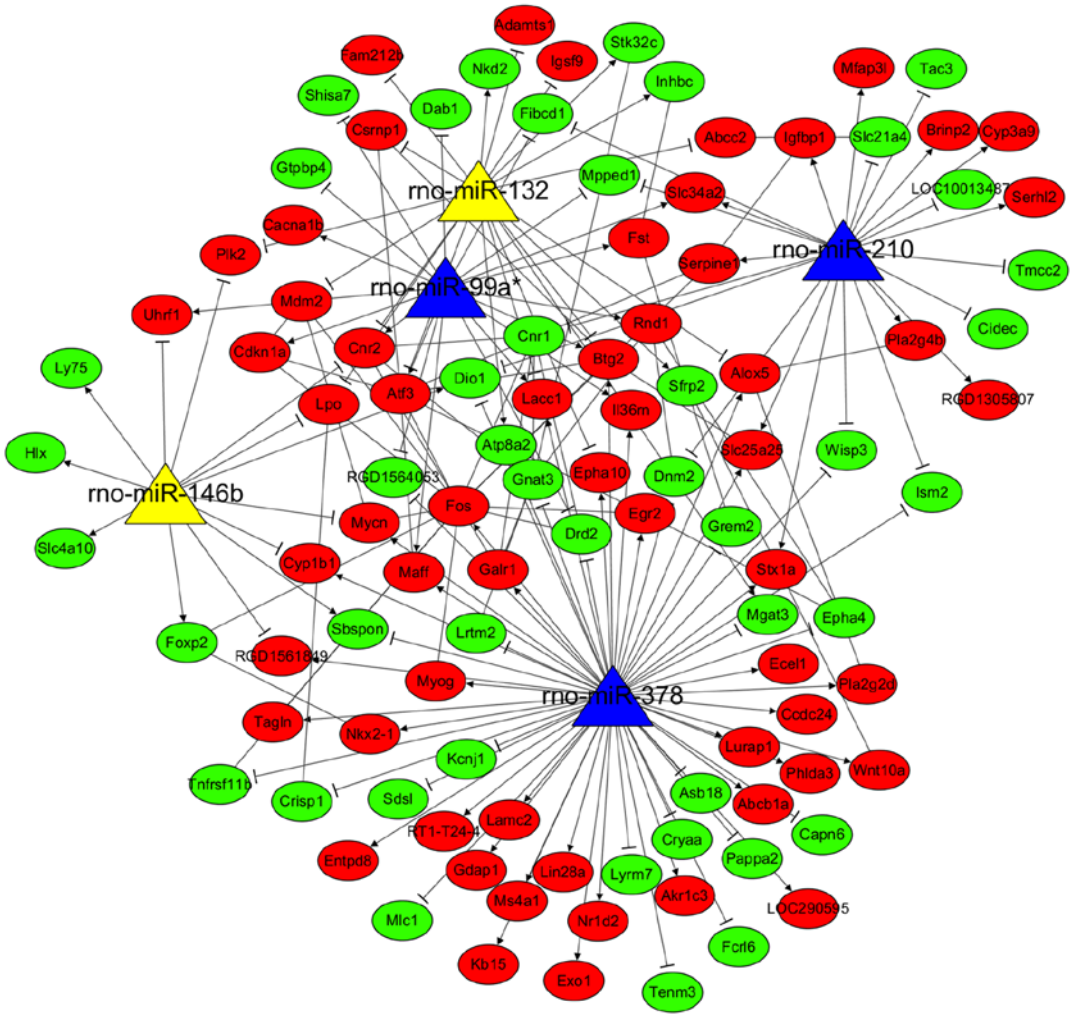

Figure 6. MSC treatment-associated miRNA-mRNA interaction network. This network was constructed using the common miRNAs between AKI vs. controls and MSC vs. AKI groups with their target genes that belonged to differentially expressed miRNAs. Red, upregulated genes; green, downregulated genes; yellow, upregulated miRNAs; blue, downregulated miRNAs. The expression level of miRNAs was defined according to the trend between AKI and control. Arrows indicate similar expression trends between miRNAs and target genes, while lines indicate opposite expression trends between miRNAs and target genes. MSC, mesenchymal stem cell; miRNA, microRNA; AKI, acute kidney injury.

notable association with identified key genes are included in Tables IV and V.

Small molecule drugs similar to MSC treatment. After uploading the DEGs into the CMAP database, 48 small molecule chemicals were predicted, including 29 with positive and 19 with negative mean and enrichment scores. The top small molecules with positive enrichment scores >0.9 may induce the development of AKI similar to cisplatin, such as ciclopirox and arachidonyltrifluoromethane (Table VI). By contrast, the top small molecules with negative enrichment scores <-0.9 may have potential effects similar to MSCs for treatment of AKI, or may exert a synergistic effect with MSCs, such as gliclazide (Table VI).

Discussion

The present study identified five miRNAs (rno-miR-378, rno-miR-210, rno-miR-99a*, rno-miR-146b and rno-miR-132) that were differentially expressed in the AKI model group compared with control group, and that were reversed following MSC treatment. Among them, two miRNAs (rno-miR-210 and rno-miR-378) could regulate hub genes (Fos, Serpine1) differentially expressed in AKI, and could affect regulation of inflammation and cell apoptosis.

Serpine1 is a gene that encodes a plasminogen activator inhibitor-1 (PAI-1). Upregulation of PAI-1 may inhibit fibrinolysis and promote renal interstitial fibrosis, which is a pathological characteristic of AKI (28,29). Furthermore, it has been reported that PAI-1 expression was increased accompanied with exaggeration of renal inflammatory injury [exhibiting high expression of nuclear factor (NF)-κB, tumor necrosis factor (TNF)-α, interleukin (IL)-6 and monocyte chemotactic protein-1] (30,31), whereas PAI-1 knockdown markedly reduced the production of the aforementioned proinflammatory cytokines, and protected mice against severe AKI and renal apoptosis (32). Elevated plasma PAI-1 levels were also revealed to be an independent factor associated with the risk of AKI (odds ratio=2.08; 95% CI: 1.42-3.05, P<0.001) following adjustment for demographics, interventions and severity of illness (33). Consistent with these studies, the present study also demonstrated that the Serpine1 gene was

Table IV. Function enrichment analysis for genes in acute kidney injury-associated miRNA-mRNA network.

Category	Term	P-value	Genes involved
KEGG	rno04721:Synaptic vesicle cycle	$4.44x10^{-3}$	STX1A, STX1B, CACNA1B, DNM2
KEGG	rno05030:Cocaine addiction	$2.53x10^{-2}$	PPP1R1B, DRD2, FOSB
KEGG	rno05031:Amphetamine addiction	$4.65x10^{-2}$	STX1A, PPP1R1B, FOSB
GO BP	GO:0043278~response to morphine	$7.20x10^{-5}$	ABCB1A, DRD2, CNR1, MDM2, FOSB
GO BP	GO:0042493~response to drug	$1.43x10^{-3}$	CDKN1A, HAVCR1, DAB1, CYP1A1, ABCB1A, DRD2, MDM2, FOSB, SLCO1A6, FOSL1
GO BP	GO:0008284~positive regulation of cell proliferation	$4.01x10^{-2}$	AKR1C3, ATF3, CLCF1, HLX, CLU, LAMC2, TIMP1, MYCN, CXCL10
GO BP	GO:0010033~response to organic substance	$7.50x10^{-3}$	CDKN1A, CYP1B1, CYP1A1, ABCB1A, TIMP1
GO BP	GO:0051412~response to corticosterone	$2.01x10^{-2}$	CDKN1A, FOSB, FOSL1
GO BP	GO:0043066~negative regulation of apoptotic process	$4.77x10^{-2}$	IER3, CDKN1A, CLU, MDM2, NQO1, CYR61, TIMP1

KEGG, Kyoto encyclopedia of genes and genomes; GO, Gene ontology; BP, biological process. Top enriched terms or terms enriched by crucial genes are listed.

Table V. Function enrichment analysis for genes in mesenchymal stem cell treatment-associated miRNA-mRNA network.

Category	Term	P-value	Genes involved
KEGG	rno00591:Linoleic acid metabolism	$2.42x10^{-2}$	CYP3A9, PLA2G4B, PLA2G2D
KEGG	rno05166:HTLV-I infection	$2.77x10^{-2}$	WNT10A, FOS, CDKN1A, ATF3, EGR2, RT1-T24-4
KEGG	rno04913:Ovarian steroidogenesis	$4.30x10^{-2}$	CYP1B1, ALOX5, PLA2G4B
GO BP	GO:0035914~skeletal muscle cell differentiation	$6.00x10^{-6}$	MAFF, FOS, ATF3, EGR2, BTG2, MYOG
GO BP	GO:0030336~negative regulation of cell migration	$1.45x10^{-4}$	GTPBP4, CYP1B1, SFRP2, DRD2, SERPINE1, NKX2-1
GO BP	GO:0042493~response to drug	$1.12x10^{-3}$	FOS, CDKN1A, TNFRSF11B, DAB1, ABCB1A, CRYAA, SFRP2, DRD2, MDM2, ABCC2
GO BP	GO:0032496~response to lipopolysaccharide	$1.22x10^{-2}$	FOS, TNFRSF11B, CNR1, SERPINE1, CNR2, NKX2-1
GO BP	GO:0033602~negative regulation of dopamine secretion	$2.91x10^{-2}$	DRD2, CNR1
GO BP	GO:0033629~negative regulation of cell adhesion mediated by integrin	$2.91x10^{-2}$	CYP1B1, SERPINE1

KEGG, kyoto encyclopedia of genes and genomes; GO, gene ontology; BP, biological process. Top enriched terms or terms enriched by crucial genes are listed.

significantly upregulated in kidney tissues of cisplatin-induced AKI and was enriched into the GO term "response to cytokine". Thus, inhibition of SERPINA1 may be a potential method to alleviate renal injury induced by cisplatin.

c-Fos is a component of the dimeric transcription factor activator protein-1 (AP-1) which is composed of various combinations of Fos (c-Fos, FosB, Fra-1 and Fra-2) and Jun (c-Jun, JunB and JunD) proteins (34). Fos/AP-1 directly controls the transcription of inflammatory cytokines (such as TNF-α, IL-1β and IL-6) by binding to their promoters, leading to their high expression and inducing AKI. The administration of Fos/AP-1 inhibitor has been confirmed to inhibit the increase in these cytokine levels in an endotoxin-induced AKI model (35,36). In accordance with these studies, the present study also demonstrated that Fos was significantly upregulated in kidney tissues of cisplatin-induced AKI.

It has been demonstrated that miRNAs induce silencing of their target genes via binding to the 3'-UTR. Thus, expression of miRNAs was also investigated in the present study. By integrating the miRNA and mRNA expression data, the results revealed that the downregulation of miR-210 may be a potential mechanism resulting in the upregulation of Serpine1 in cisplatin-induced AKI. Although their regulatory relationship has not been previously demonstrated in the literature,

Table VI. Small molecule drugs.

CMAP name	Mean	N	Enrichment	P-value	%non-null
Gliclazide	-0.63	4	-0.90	$1.60x10^{-4}$	100
Cyproterone	-0.65	4	-0.88	$5.20x10^{-4}$	100
Metacycline	-0.62	4	-0.87	$6.20x10^{-4}$	100
Ginkgolide A	-0.62	4	-0.86	$6.60x10^{-4}$	100
Estriol	-0.63	4	-0.83	$1.77x10^{-3}$	100
Adrenosterone	-0.54	4	-0.82	$2.07x10^{-3}$	100
Zimeldine	-0.57	5	-0.79	$7.80x10^{-4}$	100
H-7	-0.54	4	-0.78	$5.11x10^{-3}$	100
Tetramisole	-0.59	4	-0.76	$6.76x10^{-3}$	100
Beclometasone	-0.40	3	-0.75	$3.03x10^{-2}$	66
Aminocaproic acid	-0.42	3	-0.74	$3.67x10^{-2}$	66
Nicotinic acid	-0.50	4	-0.72	$1.20x10^{-2}$	75
Oxybuprocaine	-0.40	4	-0.68	$2.38x10^{-2}$	75
Adipiodone	-0.43	4	-0.68	$2.46x10^{-2}$	75
Tiabendazole	-0.48	4	-0.68	$2.50x10^{-2}$	75
Nabumetone	-0.52	4	-0.67	$2.69x10^{-2}$	75
Prestwick-1084	-0.54	4	-0.67	$2.84x10^{-2}$	75
Cyclopentolate	-0.48	4	-0.66	$2.98x10^{-2}$	75
Sulfametoxydiazine	-0.49	4	-0.65	$3.12x10^{-2}$	75
Hydrocotarnine	-0.50	4	-0.64	$4.23x10^{-2}$	75
Rimexolone	-0.51	4	-0.62	$4.99x10^{-2}$	75
Phthalylsulfathiazole	-0.45	5	-0.58	$3.75x10^{-2}$	60
3-acetylcoumarin	-0.45	5	-0.58	$3.79x10^{-2}$	80
Pirenzepine	-0.41	5	-0.57	$4.72x10^{-2}$	80
Sulindac	0.47	7	0.58	$9.36x10^{-3}$	71
Thiamazole	0.42	6	0.61	$1.17x10^{-2}$	66
Colistin	0.45	4	0.64	$4.28x10^{-2}$	75
Etoposide	0.48	4	0.66	$2.99x10^{-2}$	75
Adenosine phosphate	0.45	4	0.66	$2.97x10^{-2}$	75
Viomycin	0.50	4	0.66	$2.93x10^{-2}$	75
Biperiden	0.48	5	0.67	$1.05x10^{-2}$	80
Iohexol	0.53	4	0.68	$2.25x10^{-2}$	75
Atractyloside	0.54	5	0.71	$5.09x10^{-3}$	80
Ramifenazone	0.41	4	0.76	$6.15x10^{-3}$	75
Hexetidine	0.53	4	0.79	$3.64x10^{-3}$	75
Metixene	0.53	4	0.81	$2.53x10^{-3}$	75
Eticlopride	0.55	4	0.81	$2.27x10^{-3}$	100
Cefmetazole	0.75	4	0.82	$1.83x10^{-3}$	100
Lasalocid	0.66	4	0.85	$8.60x10^{-4}$	100
Penbutolol	0.59	3	0.85	$6.23x10^{-3}$	100
STOCK1N-35696	0.62	2	0.87	$3.49x10^{-2}$	100
Atracurium besilate	0.62	3	0.89	$3.08x10^{-3}$	100
Arachidonyltrifluoromethane	0.62	2	0.91	$1.84x10^{-2}$	100
Ciclopirox	0.68	4	0.91	$6.00x10^{-5}$	100

CMAP, connectivity map.

studies on the roles of miR-210 in AKI and inflammation may indirectly explain the present results. Aguado-Fraile *et al* (37) observed that miR-210-3p was significantly lower expressed in AKI patients and correlated with AKI severity. Using *in vitro* experiments, Liu *et al* (38) demonstrated that over-expression of miR-210 significantly attenuated apoptosis

in renal tubular cells, while miR-210 knockdown exerted the opposite effects. Furthermore, it was also observed that transfection with miR-210 mimic inhibited pro-inflammatory cytokine production (such as IL-4, IL-1β, IL-6 and TNF-α), cell viability reduction and cell apoptosis in chondrocytes (39) or cytotrophoblasts (40). Accordingly, it can be speculated that downregulated miR-210 may be involved in cisplatin-induced AKI by upregulating Serpine1 and then inducing cell apoptosis. This hypothesis needs to be validated by future experimental confirmation. A previous study revealed that c-Fos may be a target gene for miR-155. Treatment with cisplatin of miR-155$^{(-/-)}$ mice triggered a significantly higher level of kidney injury accompanied with significantly higher levels of c-Fos mRNA and protein (41). However, studies of miRNAs regulating Fos in AKI remain rare. In the present study, the results predicted that Fos can also be regulated by miR-378. To date, no study has explored the roles of miR-378 in AKI, but a recent report implied that miR-378 was downregulated in diabetic nephropathy and inhibition of miR-378 promoted the apoptosis of podocytes (42). This finding may indirectly indicate the anti-apoptotic roles of miR-378 in AKI, which would agree with our inflammation-apoptosis hypothesis for AKI. However, the relationship between miR-378 and Fos in AKI requires further experimental validation.

Previous studies have investigated the miRNAs that may underlie the mechanisms of MSC treatment in AKI, including miR-146 (18), miR-30 (43), miR-101 (44), miR-880, miR-141, miR-377, and miR-21 (19). In the present study, the microarray data generated by Zhu *et al* (18) were used and further screened for crucial miRNAs by integrating with the mRNA expression data from an AKI model. The present study, for the first time, demonstrated that downregulation of miR-210 and miR-378 may be key mechanisms of action of the MSC treatment in AKI. However, these findings will need to be validated by further experiments in the future.

In addition to the mechanisms of MSC treatment, the present study also predicted that gliclazide may be a potential drug to protect against AKI. Previous studies may support this hypothesis, showing that intraperitoneal injection of gliclazide reduced the levels of serum creatinine, blood urea nitrogen and microalbuminuria in diabetic rats and lessened diabetic nephropathy (45,46). The molecular mechanism of gliclazide was suggested to suppress the endoplasmic reticulum response (45) or oxidative stress (47). Thus, it can be speculated that gliclazide may be used alone or in combination with MSCs to treat cisplatin-induced AKI.

In conclusion, the present study revealed that MSCs and gliclazide may be effective for treatment of cisplatin-induced AKI by regulating miR-210/Serpine1 and miR-378/Fos-mediated inflammation. Further investigations using cell lines, animals models and clinical samples are warranted to confirm these conclusions.

Acknowledgements

Not applicable.

Funding

No funding was received.

Availability of data and materials

The microarray data GSE85957 and GSE66761 were downloaded from the GEO database in NCBI (http://www.ncbi.nlm.nih.gov/geo/).

Authors' contributions

CMZ and HLY were involved in the design of the study. CMZ, PYM and ZYZ collected the data and performed the bioinformatics analyses. NJ, DDL and PFH contributed to the acquisition and interpretation of data. CMZ and HLY drafted and revised the manuscript. All authors read and approved the final manuscript.

Ethics approval and consent to participate

Not applicable.

Patient consent for publication

Not applicable.

Competing interests

The authors declare that they have no competing interests.

References

1. Dasari S and Tchounwou PB: Cisplatin in cancer therapy: Molecular mechanisms of action. Eur J Pharmacol 740: 364-378, 2014.
2. Florea AM and Büsselberg D: Cisplatin as an anti-tumor drug: Cellular mechanisms of activity, drug resistance and induced side effects. Cancers (Basel) 3: 1351-1371, 2011.
3. Bhat ZY, Cadnapaphornchai P, Ginsburg K, Sivagnanam M, Chopra S, Treadway CK, Lin HS, Yoo G, Sukari A and Doshi MD: Understanding the risk factors and long-term consequences of cisplatin-associated acute kidney injury: An observational cohort study. PLoS One 10: e0142225, 2015.
4. Faig J, Haughton M, Taylor RC, D'Agostino RB Jr, Whelen MJ, Porosnicu Rodriguez KA, Bonomi M, Murea M and Porosnicu M: Retrospective analysis of cisplatin nephrotoxicity in patients with head and neck cancer receiving outpatient treatment with concurrent high-dose cisplatin and radiotherapy. Am J Clin Oncol 41: 432-440, 2018.
5. Saleena UV, Athiyaman MS, Vadhiraja BM, Fernandes DJ, Prabhu R and Nalini K: Evaluation of urinary tubular enzymes for the detection of early kidney injury due to cisplatin chemotherapy. Int J Biol Med Res 3: 2241-2246, 2012.
6. Peres LA, da Cunha AD Jr, Assumpção RA, Schäfer A Jr, da Silva AL, Gaspar AD, Scarpari DF, Alves JB, Girelli Neto R and de Oliveira TF: Evaluation of the cisplatin nephrotoxicity using the urinary neutrophil gelatinase-associated lipocalin (NGAL) in patients with head and neck cancer. J Bras Nefrol 36: 280-288, 2014 (In Portuguese).
7. Ozkok A and Edelstein CL: Pathophysiology of cisplatin-induced acute kidney injury. Biomed Res Int 2014: 967826, 2014.
8. Simovic Markovic B, Gazdic M, Arsenijevic A, Jovicic N, Jeremic J, Djonov V, Arsenijevic N, Lukic ML and Volarevic V: Mesenchymal stem cells attenuate cisplatin-induced nephrotoxicity in iNOS-dependent manner. Stem Cells Int 2017: 1315378, 2017.
9. Elhusseini FM, Saad MA, Anber N, Elghannam D, Sobh MA, Alsayed A, El-Dusoky S, Sheashaa H, Abdel-Ghaffar H and Sobh M: Long term study of protective mechanisms of human adipose derived mesenchymal stem cells on cisplatin induced kidney injury in sprague-dawley rats. J Stem Cells Regen Med 12: 36-48, 2016.
10. Lee SJ, Ryu MO, Seo MS, Park SB, Ahn JO, Han SM, Kang KS, Bhang DH and Youn HY: Mesenchymal stem cells contribute to improvement of renal function in a canine kidney injury model. In Vivo 31: 1115-1124, 2017.

11. Moghadasali R, Mutsaers HA, Azarnia M, Aghdami N, Baharvand H, Torensma R, Wilmer MJ and Masereeuw R: Mesenchymal stem cell-conditioned medium accelerates regeneration of human renal proximal tubule epithelial cells after gentamicin toxicity. Exp Toxicol Pathol 65: 595-600, 2013.
12. Park JH, Jang HR, Kim DH, Kwon GY, Lee JE, Huh W, Choi SJ, Oh W, Oh HY and Kim YG: Early, but not late, treatment with human umbilical cord blood-derived mesenchymal stem cells attenuates cisplatin nephrotoxicity through immunomodulation. Am J Physiol Renal Physiol 313: F984-F996, 2017.
13. Sherif IO, Almutabagani LA, Alnakhli AM, Sobh MA and Mohammed HE: Renoprotective effects of angiotensin receptor blocker and stem cells in acute kidney injury: Involvement of inflammatory and apoptotic markers. Exp Biol Med (Maywood) 240: 1572-1579, 2015.
14. Liao W, Fu Z, Zou Y, Wen D, Ma H, Zhou F, Chen Y, Zhang M and Zhang W: MicroRNA-140-5p attenuated oxidative stress in Cisplatin induced acute kidney injury by activating Nrf2/ARE pathway through a Keap1-independent mechanism. Exp Cell Res 360: 292-302, 2017.
15. Lee CG, Kim JG, Kim HJ, Kwon HK, Cho IJ, Choi DW, Lee WH, Kim WD, Hwang SJ, Choi S and Kim SG: Discovery of an integrative network of microRNAs and transcriptomics changes for acute kidney injury. Kidney Int 86: 943-953, 2014.
16. Guo Y, Ni J, Chen S, Bai M, Lin J, Ding G, Zhang Y, Sun P, Jia Z, Huang S, *et al*: MicroRNA-709 mediates acute tubular injury through effects on mitochondrial function. J Am Soc Nephrol 29: 449-461, 2018.
17. Qin W, Xie W, Yang X, Xia N and Yang K: Inhibiting microRNA-449 attenuates cisplatin-induced injury in NRK-52E cells possibly via regulating the SIRT1/P53/BAX pathway. Med Sci Monit 22: 818-823, 2016.
18. Zhu Y, Yu J, Yin L, Zhou Y, Sun Z, Jia H, Tao Y, Liu W, Zhang B, Zhang J, *et al*: MicroRNA-146b, a sensitive indicator of mesenchymal stem cell repair of acute renal injury. Stem Cells Transl Med 5: 1406-1415, 2016.
19. de Almeida DC, Bassi ÊJ, Azevedo H, Anderson L, Origassa CS, Cenedeze MA, de Andrade-Oliveira V, Felizardo RJ, da Silva RC, Hiyane MI, *et al*: A regulatory miRNA-mRNA network is associated with tissue repair induced by mesenchymal stromal cells in acute kidney injury. Front Immunol 7: 645, 2017.
20. Pavkovic M, Riefke B and Ellinger-Ziegelbauer H: Urinary microRNA profiling for identification of biomarkers after cisplatin-induced kidney injury. Toxicology 324: 147-157, 2014.
21. Pavkovic M, Riefke B, Gutberlet K, Raschke M and Ellinger-Ziegelbauer H: Comparison of the MesoScale discovery and Luminex multiplex platforms for measurement of urinary biomarkers in a cisplatin rat kidney injury model. J Pharmacol Toxicol Methods 69: 196-204, 2014.
22. Irizarry RA, Hobbs B, Collin F, Beazer-Barclay YD, Antonellis KJ, Scherf U and Speed TP: Exploration, normalization, and summaries of high density oligonucleotide array probe level data. Biostatistics 4: 249-264, 2003.
23. Ritchie ME, Phipson B, Wu D, Hu Y, Law CW, Shi W and Smyth GK: limma powers differential expression analyses for RNA-sequencing and microarray studies. Nucleic Acids Res 43: e47, 2015.
24. Szklarczyk D, Franceschini A, Wyder S, Forslund K, Heller D, Huerta-Cepas J, Simonovic M, Roth A, Santos A, Tsafou KP, *et al*: STRING v10: Protein-protein interaction networks, integrated over the tree of life. Nucleic Acids Res 43 (Database Issue): D447-D452, 2015.
25. Kohl M, Wiese S and Warscheid B: Cytoscape: Software for visualization and analysis of biological networks. Methods Mol Biol 696: 291-303, 2011.
26. Bader GD and Hogue CW: An automated method for finding molecular complexes in large protein interaction networks. BMC Bioinformatics 4: 2, 2003.
27. Dweep H and Gretz N: miRWalk2.0: A comprehensive atlas of microRNA-target interactions. Nat Methods 12: 697, 2015.
28. Zhang W, Sha Y, Wei K, Wu C, Ding D, Yang Y, Zhu C, Zhang Y, Ding G, Zhang A, *et al*: Rotenone ameliorates chronic renal injury caused by acute ischemia/reperfusion. Oncotarget 9: 24199-24208, 2018.
29. Eren M, Place AT, Thomas PM, Flevaris P, Miyata T and Vaughan DE: PAI-1 is a critical regulator of FGF23 homeostasis. Sci Adv 3: e1603259, 2017.
30. Xue HY, Yuan L, Cao YJ, Fan YP, Chen XL and Huang XZ: Resveratrol ameliorates renal injury in spontaneously hypertensive rats by inhibiting renal micro-inflammation. Biosci Rep 36: pii: e00339, 2016.
31. Jesmin S, Gando S, Zaedi S, Prodhan SH, Sawamura A, Miyauchi T, Hiroe M and Yamaguchi N: Protease-activated receptor 2 blocking peptide counteracts endotoxin-induced inflammation and coagulation and ameliorates renal fibrin deposition in a rat model of acute renal failure. Shock 32: 626-632, 2009.
32. Gupta KK, Donahue DL, Sandoval-Cooper MJ, Castellino FJ and Ploplis VA: Abrogation of plasminogen activator inhibitor-1-vitronectin interaction ameliorates acute kidney injury in murine endotoxemia. PLoS One 10: e0120728, 2015.
33. Liu KD, Glidden DV, Eisner MD, Parsons PE, Ware LB, Wheeler A, Korpak A, Thompson BT, Chertow GM and Matthay MA; National Heart, Lung, and Blood Institute ARDS Network Clinical Trials Group: Predictive and pathogenetic value of plasma biomarkers for acute kidney injury in patients with acute lung injury. Crit Care Med 35: 2755-2761, 2007.
34. Angel P and Karin M: The role of Jun, Fos and the AP-1 complex in cell-proliferation and transformation. Biochim Biophys Acta 1072: 129-157, 1991.
35. Miyazaki H, Morishita J, Ueki M, Nishina K, Shiozawa S and Maekawa N: The effects of a selective inhibitor of c-Fos/activator protein-1 on endotoxin-induced acute kidney injury in mice. BMC Nephrol 13: 153, 2012.
36. Ishida M, Ueki M, Morishita J, Ueno M, Shiozawa S and Maekawa N: T-5224, a selective inhibitor of c-Fos/activator protein-1, improves survival by inhibiting serum high mobility group box-1 in lethal lipopolysaccharide-induced acute kidney injury model. J Intensive Care 3: 49, 2015.
37. Aguado-Fraile E, Ramos E, Conde E, Rodríguez M, Martín-Gómez L, Lietor A, Candela Á, Ponte B, Liaño F and García-Bermejo ML: A pilot study identifying a set of microRNAs as precise diagnostic biomarkers of acute kidney injury. PLoS One 10: e0127175, 2015.
38. Liu LL, Li D, He YL, Zhou YZ, Gong SH, Wu LY, Zhao YQ, Huang X, Zhao T, Xu L, *et al*: miR-210 protects renal cell against hypoxia-induced apoptosis by targeting HIF-1 alpha. Mol Med 23: 258-271, 2017.
39. Zhang D, Cao X, Li J and Zhao G: MiR-210 inhibits NF-κB signaling pathway by targeting DR6 in osteoarthritis. Sci Rep 5: 12775, 2015.
40. Kopriva SE, Chiasson VL, Mitchell BM and Chatterjee P: TLR3-induced placental miR-210 down-regulates the STAT6/interleukin-4 pathway. PLoS One 8: e67760, 2013.
41. Pellegrini KL, Han T, Bijol V, Saikumar J, Craciun FL, Chen WW, Fuscoe JC and Vaidya VS: MicroRNA-155 deficient mice experience heightened kidney toxicity when dosed with cisplatin. Toxicol Sci 141: 484-492, 2014.
42. Lei X, Zhang BD, Ren JG and Luo FL: Astragaloside suppresses apoptosis of the podocytes in rats with diabetic nephropathy via miR-378/TRAF5 signaling pathway. Life Sci 206: 77-83, 2018.
43. Gu D, Zou X, Ju G, Zhang G, Bao E and Zhu Y: Mesenchymal stromal cells derived extracellular vesicles ameliorate acute renal ischemia reperfusion injury by inhibition of mitochondrial fission through miR-30. Stem Cells Int 2016: 2093940, 2016.
44. Liu J, Hua R, Gong Z, Shang B, Huang Y, Guo L, Liu T and Xue J: Human amniotic epithelial cells inhibit CD4+ T cell activation in acute kidney injury patients by influencing the miR-101-c-Rel-IL-2 pathway. Mol Immunol 81: 76-84, 2017.
45. Zhang YW, Wang X, Ren X and Zhang M: Involvement of glucose-regulated protein 78 and spliced X-box binding protein 1 in the protective effect of gliclazide in diabetic nephropathy. Diabetes Res Clin Pract 146: 41-47, 2018.
46. Ezel T, Kocyigit Y, Deveci E, Atamer Y, Sermet A, Uysal E, Aktaş A and Yavuz D: Biochemical and histopathological investigation of resveratrol, gliclazide, and losartan protective effects on renal damage in a diabetic rat model. Anal Quant Cytopathol Histpathol 37: 187-198, 2015.
47. Onozato ML, Tojo A, Goto A and Fujita T: Radical scavenging effect of gliclazide in diabetic rats fed with a high cholesterol diet. Kidney Int 65: 951-960, 2004.